

Supplementary Materials

Probing the reactivity of [4Fe-4S] FNR with O₂ and NO: increased O₂ resistance and relative specificity for NO of the [4Fe-4S] L28H FNR cluster

Jason C. Crack, Patricia Amara, Eve de Rosny, Claudine Darnault, Melanie R. Stapleton, Jeffrey Green, Anne Volbeda, Juan C. Fontecilla-Camps and Nick E. Le Brun

Supplementary Figures

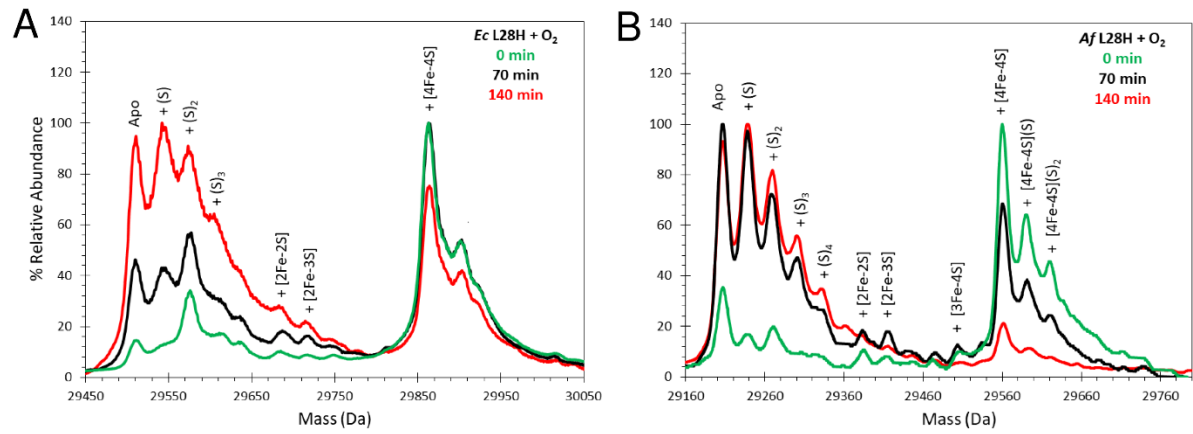


Figure S1. Reaction of L28H-EcFNR and L28H-A/FNR with O₂ monitored by native MS. Deconvoluted mass spectrum of (A) L28H-EcFNR and (B) L28H-A/FNR before (green line) and after (70 min, black line; 140 min, red line) exposure to O₂. Persulfide adducts of the apo proteins are the major products observed.

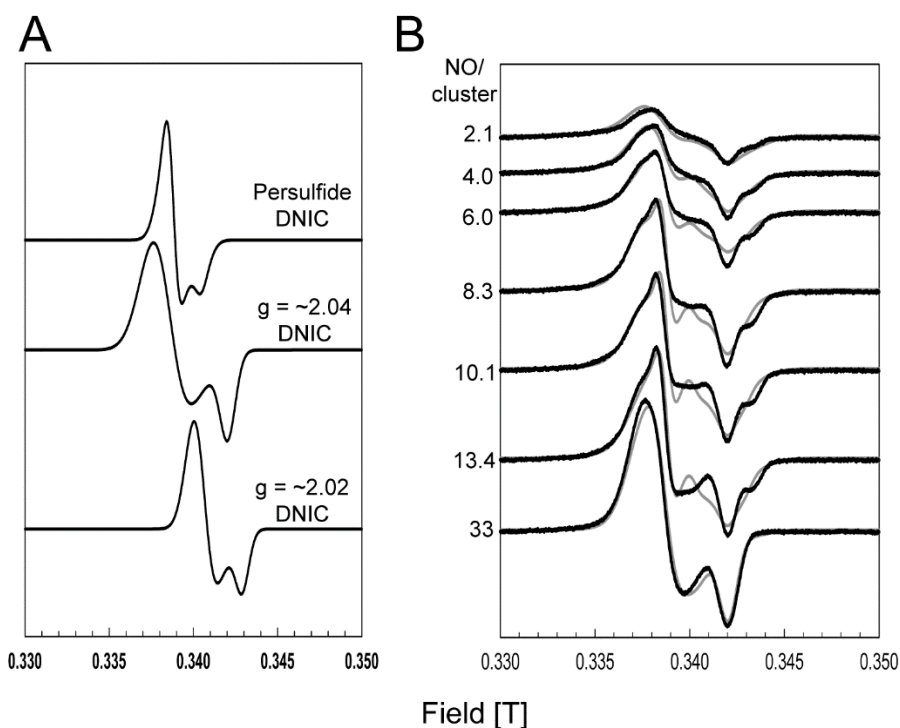


Figure S2. Deconvolution of EPR spectra resulting from nitrosylation of [4Fe-4S] L28H-EcFNR. (A), Simulated EPR spectra of persulfide-ligated DNIC ($g_{\perp} = 2.044$, $g_{\parallel} = 2.032$) [50,60], and two thiol-coordinated DNICs at $g \approx 2.04$ ($g_{\perp} = 2.045$, $g_{\parallel} = 2.023$) [61,62], and $g \approx 2.02$ ($g_{\perp} = 2.023$, $g_{\parallel} = 2.016$) [28,63] that were used to deconvolute the recorded (74 K) EPR spectra in (B). (B), EPR spectra for nitrosylated L28H-EcFNR (data, black lines), together with simulations of the experimental data ($R^2 \approx 0.90$) (gray lines) obtained by the combination of varying amounts of the spectra shown in A.

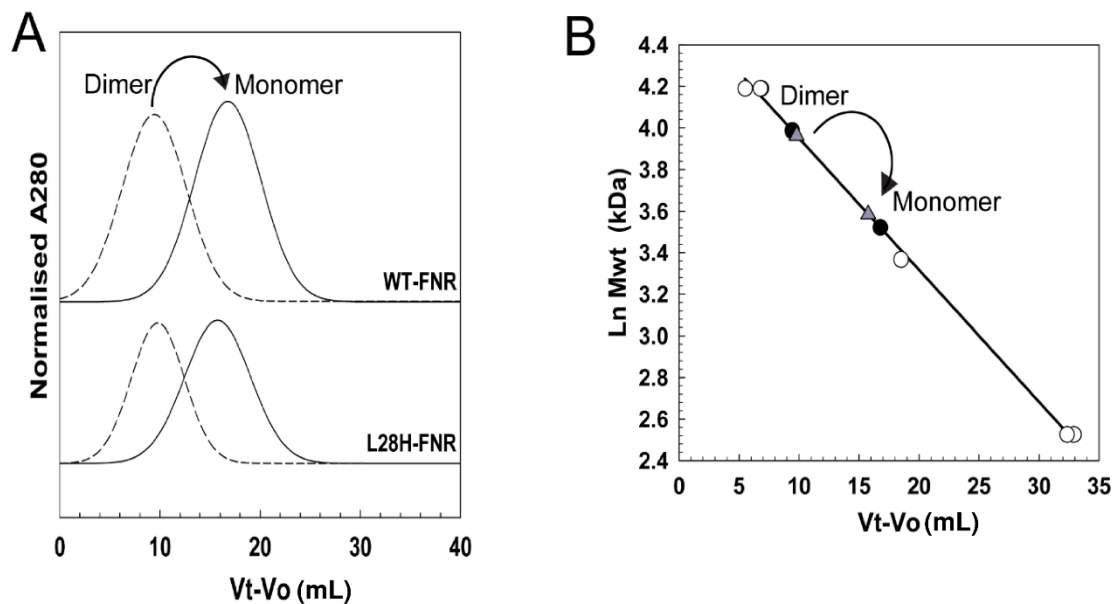


Figure S3. Gel filtration of [4Fe-4S]- L28H-EcFNR before and after nitrosylation. (A) Chromatogram for L28H-EcFNR pre- (dashed line) and post-NO exposure (solid black line). (B) Standard calibration curve for Sephacryl S100HR column. White circles correspond to standard proteins (BSA, carbonic anhydrase, cytochrome *c*). Grey triangles correspond to L28H-EcFNR (pre-NO, 53 kDa; post-NO, 37 kDa), respectively. Black circles correspond to wt-EcFNR (see [24] for further details). The data indicate that nitrosylation of [4Fe-4S]-L28H-EcFNR results in an iron-nitrosyl bound FNR monomer. V_o is the void volume of the column; V_t is the total elution volume, including void volume.

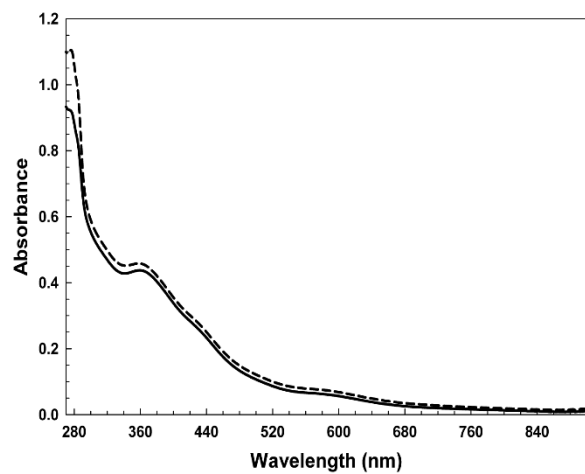


Figure S4. UV-visible properties of nitrosylated [4Fe-4S] L28H-EcFNR. Absorbance spectrum of nitrosylated L28H-EcFNR (dashed black line) after rapid gel filtration (PD10, Cytiva). The samples contained ~1.4 (54 μ M) RRE per protein, based on a $\epsilon_{362 \text{ nm}}$ value of 8530 $\text{M}^{-1} \text{cm}^{-1}$ [61]. The L28H sample corresponds to sample 3 in Table 1. The previously published [24] spectrum of nitrosylated wt FNR (solid black line) is shown for comparison.

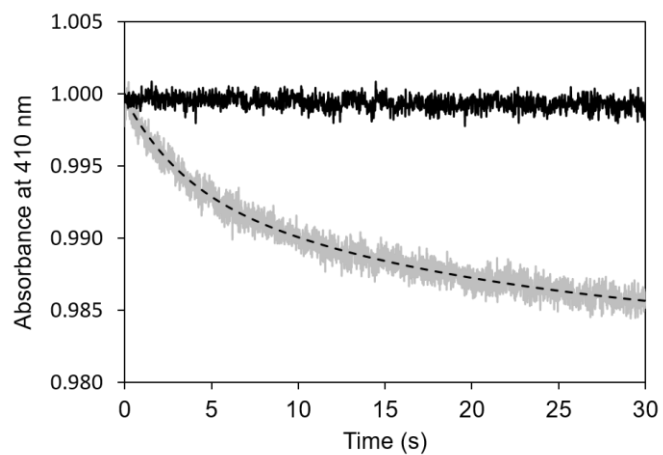


Figure S5. Reaction of [4Fe-4S]-A/FNR with O₂. Stopped-flow measurements for the wild-type (gray) and the L28H-FNR variant (black). Curves are translated to Abs_{410 nm}=1 at time 0. The dashed line represents the fit of the wild-type curve to a two-phase exponential decay equation.

Supplementary Tables

Table S1. X-ray data collection and refinement statistics for [4Fe-4S] L28H-A/FNR.

X-ray data		Refinement	
Space group	I422	Resolution (Å)	47.77-2.40
Cell dimensions		Reflections (work / free)	12080 / 568
a=b, c (Å)	75.20 217.47	R _{work} / R _{free}	19.8 / 22.2
α=β=γ (°)	90	Number of atoms	
Resolution (Å) ^a	47.8-2.4 (2.48-2.4)	Protein	1839
R _{merge} (%)	7.1 (340.8)	[4Fe-4S] cluster	8
mean(I/σ(I))	18.6 (0.7)	Solvent (MPD and water)	115
CC(1/2)	1.000 (0.449)	Average B factors (Å ²)	
Total number of observations	147841 (14671)	Protein	88.2
Total number unique	12709 (1205)	[4Fe-4S] cluster	91.0
Completeness (%)	99.9 (99.7)	Solvent	86.6
Redundancy	11.6 (12.2)	R.m.s. deviations	
Anomalous completeness (%)	99.8 (99.4)	Bond lengths (Å)	0.003
Anomalous redundancy	6.2 (6.4)	Bond angles (°)	0.53
		Ramachandran plot outliers ^b	0
		Rotamer outliers (%) ^b	1.5
		All atom clash score ^b	2.7

^a Numbers within brackets denote the highest resolution shell.

^b Molprobrity statistics [64].

Table S2. Rate constants for the nitrosylation of [4Fe-4S] L28H-*Ec*FNR with NO and comparison to wild-type FNR and Wbl proteins.

		Rate constants/ $\text{M}^{-1} \text{s}^{-1}$ ^a			
Phase	Step	WT FNR	L28H FNR	WhiD	WhiB1
1	A→B	$2.81 \pm 0.10 \times 10^5$	$1.33 \pm 0.02 \times 10^5$	6.50×10^5	4.40×10^5
2	B→C	$1.89 \pm 0.10 \times 10^4$	$1.59 \pm 0.07 \times 10^4$	2.13×10^4	1.38×10^4
3	C→D	$4.61 \pm 0.25 \times 10^3$	$9.51 \pm 0.49 \times 10^3$	5.36×10^3	8.34×10^3
4	D→E	$0.75 \pm 0.03 \times 10^3$	$1.29 \pm 0.09 \times 10^3$	1.00×10^3	0.90×10^3

^a Derived from linear fits of the data at low NO concentrations in Fig. 5. Rate constants for the nitrosylation of wild type FNR, *S. coelicolor* WhiD and *M. tuberculosis* WhiB1 [24, 28], are shown for comparison.